

Table I. Number of W mesons as a function of boson mass/ 1.2×10^{17} protons/8 tons. Branching ratio ($W \rightarrow e\nu$)/($W \rightarrow$ all) of $\frac{1}{4}$ is assumed. Detection efficiency of 60% for $e\nu$ mode is also included in this calculation.

m_W (in BeV)	Expected number of W mesons
1.5	9
1.8	4
2.0	2
2.2	1

netic-moment contribution ($\pm e/2M_W$) and allow for some of the theoretical uncertainties as well as the neutrino flux uncertainty, a boson mass of $2m_p$ would predict 3 ± 1.2 events where we see none. The result, on the basis of $\geq 90\%$ confidence level, is then

$$m_W > 2m_p.$$

This conclusion re-enforces a similar one recently obtained by the CERN group.¹² A study of the backgrounds (6), (7), and (8) leads us to believe that this limit may be extended to about 2.5 BeV using the technique described here.

We would like to thank Professor S. Taylor and the group at Stevens Institute of Technology for scanning the emulsions, and J. Hudis for assistance with the radiochemistry. The co-operation of the AGS group was essential, especially in the extraction¹³ of the external beam by Green, Raka, and Forsythe. Finally, we would like to thank Professor J. Steinberger for his collaboration during the early stages of this investigation.

*Work supported in part by the U. S. Atomic Energy Commission.

†Present address: Physics Department, Princeton University, Princeton, New Jersey.

‡Present address: Physics Department, Cornell University, Ithaca, New York.

¹G. Danby, J.-M. Gaillard, K. Goulianos, L. M. Lederman, N. Mistry, M. Schwartz, and J. Steinberger, Phys. Rev. Letters **9**, 36 (1962).

²M. M. Block, H. Burmeister, D. C. Cundy, B. Eiben, C. Franzinetti, J. Keren, R. Möllerud, G. Myatt, M. Nikolic, A. Orkin-LeCourtois, M. Paty, D. H. Perkins, C. A. Ramm, K. Schultze, H. Sletten, K. Soop, R. Stump, W. Venus, and H. Yoshiki, Phys. Letters **12**, 281 (1964); G. Bernardini, J. K. Bienlein, G. Von Dardel, H. Faissner, F. Ferrero, J. M. Gaillard, H. J. Gerber, B. Hahn, V. Kaftanov, F. Krienen, C. Manfredotti, M. Reinharz, and R. A. Salmeron, Phys. Letters **13**, 86 (1964).

³W. Czyz and J. D. Walecka, Phys. Letters **8**, 77 (1964).

⁴Alfred C. T. Wu, Chen-Ping Yang, Kurt Fuchel, and Sidney Heller, Phys. Rev. Letters **12**, 57 (1964).

⁵J. Bell and M. Veltmann, Phys. Letters **5**, 94 (1962).

⁶H. Überall, Phys. Rev. **133**, B444 (1964).

⁷We are very grateful to Professor Wu and Dr. Fuchel for extending these calculations for us up to a boson mass of 2.8 BeV.

⁸T. D. Lee and C. N. Yang, Phys. Rev. Letters **4**, 307 (1960).

⁹G. von Gehlen, Nuovo Cimento **30**, 859 (1963).

¹⁰D. E. Dorfan *et al.*, Phys. Rev. Letters **14**, 995 (1965).

¹¹For details, see R. Burns *et al.*, "Determination of Neutrino Flux," Informal Conference on Neutrino Physics, CERN, January 1965 (to be published).

¹²See reference 2. The CERN group has presented the results of more extensive data at the Informal Conference on Neutrino Physics, Geneva, January 1965 (to be published).

¹³G. T. Danby, G. K. Green, and E. C. Raka, Bull. Am. Phys. Soc. **10**, 34 (1965).

ELASTIC SCATTERING OF PROTONS, ANTIPROTONS,* NEGATIVE PIONS, AND NEGATIVE KAONS AT HIGH ENERGIES

K. J. Foley, R. S. Gilmore,† S. J. Lindenbaum, W. A. Love,
S. Ozaki, E. H. Willen, R. Yamada, and L. C. L. Yuan

Brookhaven National Laboratory, Upton, New York

(Received 4 June 1965)

This Letter reports the extension to higher energy of our previous measurements¹⁻³ of the differential cross section for elastic p - p , π^- - p , \bar{p} - p , and K^- - p scattering in the region $|t|=0.2$ to 1.0 (BeV/c)², where t is the negative square of the four-momentum transfer. The region of incident momentum covered was 15

to 26 BeV/c for π^- - p and p - p and 12 to 16 BeV/c for K^- - p and \bar{p} - p scattering, the main purpose being to investigate further the energy dependence of the differential cross sections. Above 15 BeV/c incident momentum, the p - p differential cross sections continue to shrink with increasing energy while the π^- - p differ-

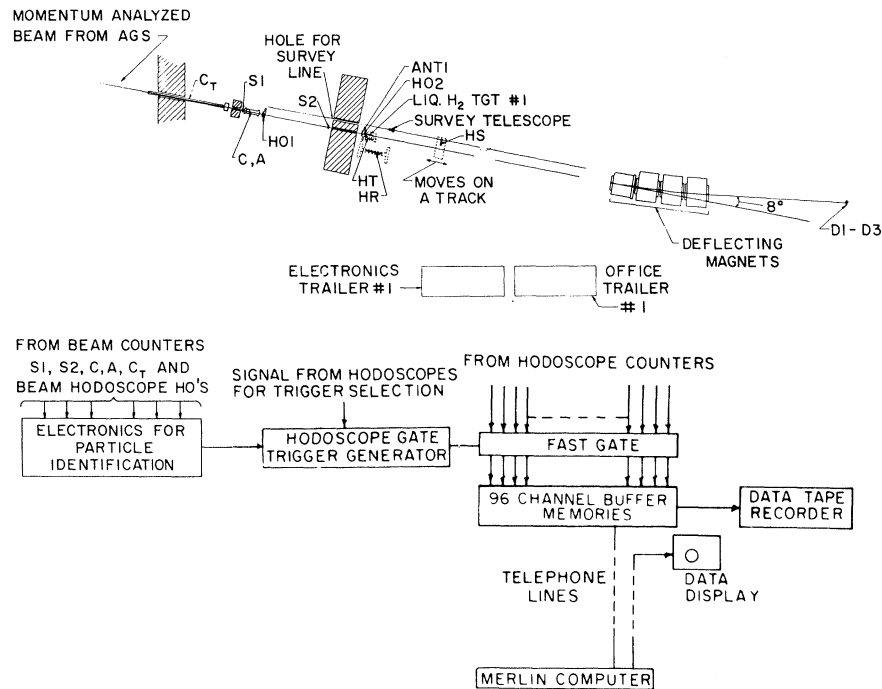


FIG. 1. The experimental arrangement.

ential cross sections are energy independent. However, in the \bar{p} - p case the diffraction pattern expands with increasing energy.

The apparatus is shown in Fig. 1. The positive beam was a 3.5° secondary beam from G10 target at the Brookhaven AGS, while the negative beam, which was brought down the same beam line by reversing all beam magnets, was produced near 0° in the G9 target section, one AGS magnet upstream. The momentum spread was measured to be $\pm 0.8\%$. The mean beam momentum was determined to $\pm 0.2\%$. The intensity varied from 10^5 particles/pulse (limited by collimation) at the lower energy to 10^3 protons/pulse or $3 \times 10^3 \pi^-$ /pulse at 26 BeV/c. The apparatus shown in Fig. 1 was very similar to that used in our previous measurements.¹ We identified elastic scattering events by measuring the angles (θ, φ) of both scattered and recoil particles. In order to cover approximately the same region of four-momentum transfer the hodoscope HS was mounted on rails and moved parallel to the beam when the momentum was changed. After each momentum change, HS was aligned to ± 0.005 in. in directions perpendicular to the beam. The resolution of the system was as follows: for polar angle of scattered particle it varied from ± 3.5 mrad at 12 BeV/c to

± 1.5 mrad at 26 BeV/c; for the azimuthal angle of the forward scattered particle it varied from ± 45 mrad at $t = 0.2$ to ± 21 mrad at $t = 1.0$ (BeV/c)²; the recoil angle resolution was ± 42 mrad in θ and ± 26 mrad in φ . Since the present measurements were made at higher incident momenta, we used a 24-ft long air-filled threshold Cherenkov counter in parallel with the differential Cherenkov counter in order to improve the separation of pions and kaons. The hodoscopes HO1 and HO2 were used to measure the incident angle to ± 0.7 mrad. The fast-gate and data-handling system, which accepted 32 events per pulse was the same as that described earlier¹; also, we again transmitted the information to Merlin computer for on-line analysis. The computer separated out the coplanar events and stored the data in eleven "scattering-angle" bins as a function of recoil angle. At the end of each run the computer subtracted the nonelastic background and calculated the differential cross sections and the values of t for each bin. The nonelastic background was $< 1\%$ at the smallest t and increased slowly with increasing $|t|$ until the data was cut off at the point of 30% background.

The results $(d\sigma/dt)/(d\sigma/dt)_{\text{opt}}$ vs $-t$ for p - p , π^- - p , K^- - p , and \bar{p} - p are shown⁴ in Fig. 2. The 15 BeV/c p - p data were used to check the

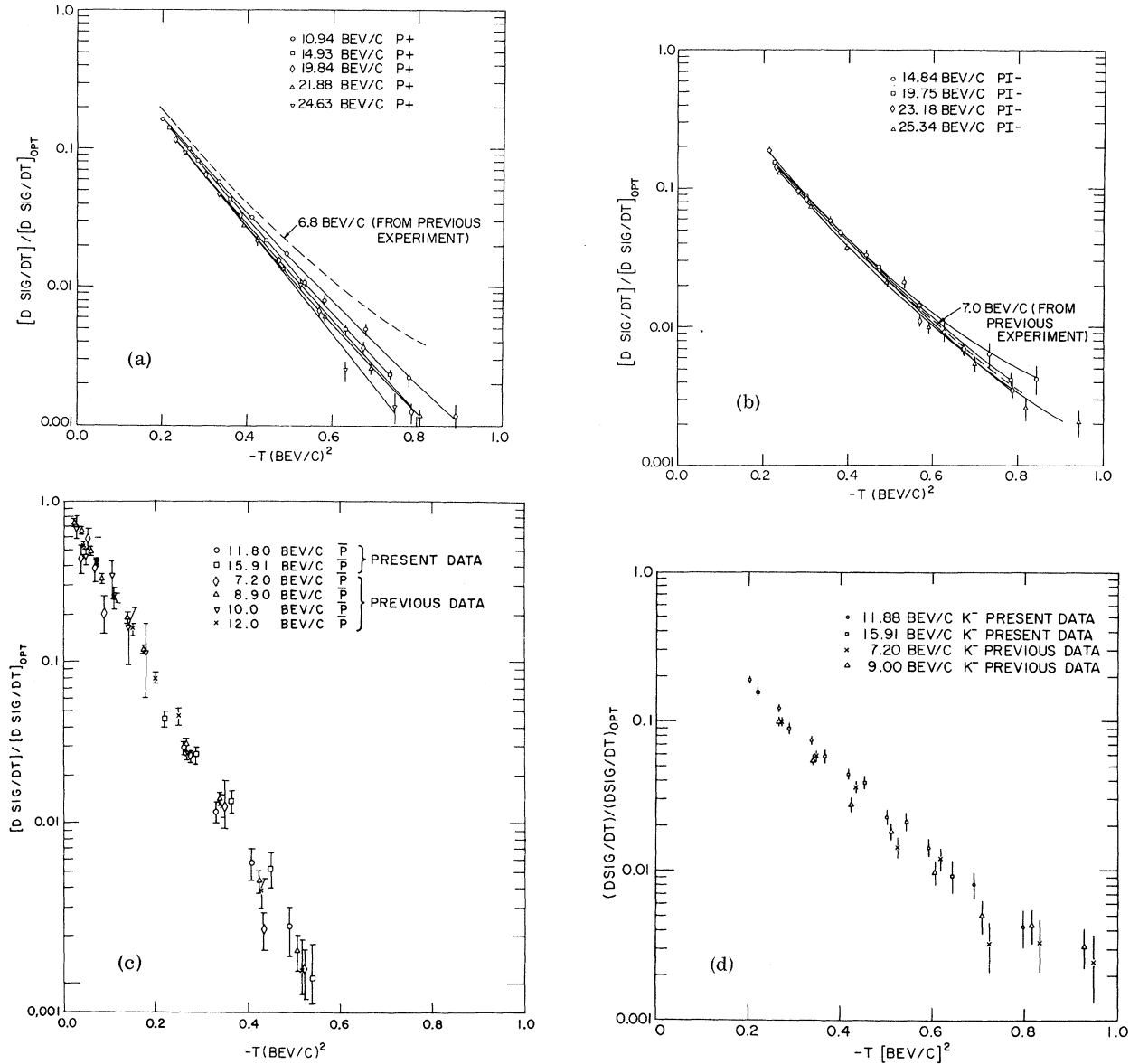


FIG. 2. $(d\sigma/dt)/(d\sigma/dt)_{\text{opt}}$ vs. $-t \text{ (BeV/c)}^2$ (a) for 11- to 25-BeV/c $p-p$ elastic scattering; (b) for 15- to 25-BeV/c π^-p elastic scattering; (c) for 7- to 16-BeV/c $\bar{p}-p$ elastic scattering; (d) for 7- to 16-BeV/c K^-p elastic scattering.

present normalization against that of the previous measurements.¹⁻³ The agreement was better than 2%. However, the two experiments used mainly the same hodoscopes, and so we estimate the limit of systematic overall scale error at $\pm 5\%$. All known effects due to finite counter sizes and finite resolutions were corrected for in an unfolding procedure which determined the resultant effective value of t for each angular bin. The errors shown include statistical errors, uncertainty in the background subtraction, and the uncertainty in calculating the effective value of $|t|$, as reflected as an

uncertainty in the cross sections, and are thus applicable point to point and momentum to momentum. The measured value of $d\sigma/dt$ vs t and errors are shown in Table I. In order to show any energy dependence more clearly, we have interpolated the data to nearby fixed values of t by fitting each curve with a function of the form $d\sigma/dt = \exp(a + bt + ct^2)$. For purposes of the fits, we have used no points with greater than 30% background for the $p-p$, $\pi-p$, and $\bar{p}-p$ data, and no points with $|t|$ greater than 0.9 $(\text{BeV/c})^2$ for K^-p . Figure 3 shows the interpolated data for $p-p$ and π^-p . The data

Table I. The measured values of the cross sections. For each momentum p are listed the center of mass energy squared s , the value of $d\sigma/dt$ at $t=0$ predicted by the optical theorem, the cross sections with errors, and the coefficients with errors of the least-squares fit to the cross sections using the expression $\exp(a+bt+ct^2)$.

P-P									
p	$= 10.94 \text{ BeV/c}$		14.93		19.84		21.88		24.63
s	$= 22.36 \text{ (BeV)}^2$		29.83		39.03		42.85		48.01
$(\frac{d\sigma}{dt})_{\text{opt}}$	$= 79.9 \text{ mb/(BeV/c)}^2$		79.9		79.9		79.9		79.9
$ t $	$d\sigma/dt$	$ t $	$d\sigma/dt$	$ t $	$d\sigma/dt$	$ t $	$d\sigma/dt$	$ t $	$d\sigma/dt$
0.200	13.19 ± 0.32	0.216	11.48 ± 0.23	0.230	9.29 ± 0.28	0.235	8.98 ± 0.28	0.254	7.56 ± 0.34
0.263	8.10 ± 0.23	0.284	6.67 ± 0.16	0.302	5.14 ± 0.19	0.309	4.82 ± 0.18	0.334	3.74 ± 0.21
0.333	4.66 ± 0.16	0.360	3.48 ± 0.10	0.383	2.64 ± 0.12	0.392	2.25 ± 0.10	0.424	1.712 ± 0.122
0.411	2.57 ± 0.11	0.444	1.752 ± 0.064	0.474	1.269 ± 0.070	0.485	1.100 ± 0.063	0.525	0.824 ± 0.074
0.493	1.411 ± 0.076	0.534	0.866 ± 0.039	0.569	0.552 ± 0.042	0.583	0.494 ± 0.038	0.632	0.203 ± 0.036
0.582	0.641 ± 0.048	0.631	0.402 ± 0.024	0.674	0.291 ± 0.030	0.691	0.209 ± 0.024	0.748	0.110 ± 0.028
0.679	0.393 ± 0.039	0.736	0.189 ± 0.016	0.787	0.100 ± 0.018	0.807	0.096 ± 0.016		
0.782	0.178 ± 0.026								
0.891	0.094 ± 0.018								
a	$= 4.25 \pm 0.09$		4.32 ± 0.10		4.19 ± 0.15		4.38 ± 0.16		4.09 ± 0.30
b	$= 8.56 \pm 0.47$		8.89 ± 0.52		8.68 ± 0.79		9.63 ± 0.78		7.97 ± 1.56
c	$= 1.20 \pm 0.54$		0.98 ± 0.62		0.70 ± 0.92		1.56 ± 0.89		0.82 ± 1.83

π^-p									
p	$= 14.84 \text{ BeV/c}$		19.75		23.18		25.34		
s	$= 28.75 \text{ (BeV)}^2$		37.96		44.40		48.45		
$(\frac{d\sigma}{dt})_{\text{opt}}$	$= 34.3 \text{ mb/(BeV/c)}^2$		33.1		32.6		32.4		
$ t $	$d\sigma/dt$	$ t $	$d\sigma/dt$	$ t $	$d\sigma/dt$	$ t $	$d\sigma/dt$	$ t $	$d\sigma/dt$
0.215	6.52 ± 0.32	0.229	5.37 ± 0.15	0.230	5.00 ± 0.16	0.238	4.50 ± 0.17		
0.282	3.33 ± 0.20	0.301	3.02 ± 0.10	0.301	2.91 ± 0.11	0.312	2.60 ± 0.12		
0.358	2.04 ± 0.14	0.382	1.686 ± 0.068	0.383	1.641 ± 0.072	0.397	1.318 ± 0.072		
0.442	1.152 ± 0.098	0.472	0.940 ± 0.046	0.473	0.897 ± 0.048	0.491	0.742 ± 0.049		
0.531	0.739 ± 0.076	0.567	0.503 ± 0.031	0.569	0.390 ± 0.029	0.590	0.351 ± 0.033		
0.627	0.328 ± 0.054	0.671	0.247 ± 0.022	0.674	0.244 ± 0.023	0.699	0.192 ± 0.024		
0.732	0.223 ± 0.045	0.784	0.148 ± 0.016	0.787	0.126 ± 0.017	0.817	0.091 ± 0.018		
0.843	0.148 ± 0.035					0.944	0.073 ± 0.015		
a	$= 3.85 \pm 0.19$		3.60 ± 0.13		3.48 ± 0.15		3.61 ± 0.15		
b	$= 10.20 \pm 0.96$		8.98 ± 0.65		8.53 ± 0.74		9.46 ± 0.71		
c	$= 4.02 \pm 1.07$		2.44 ± 0.73		1.79 ± 0.83		2.83 ± 0.72		

$\bar{p}p$				K^-p			
p	$= 11.80 \text{ BeV/c}$		15.91		11.88		15.91
s	$= 23.97 \text{ (BeV/c)}^2$		31.67		23.44		30.99
$(\frac{d\sigma}{dt})_{\text{opt}}$	$= 149.3 \text{ mb/(BeV/c)}^2$		135.8		26.8		24.6
$ t $	$d\sigma/dt$	$ t $	$d\sigma/dt$	$ t $	$d\sigma/dt$	$ t $	$d\sigma/dt$
0.199	10.61 ± 0.87	0.219	6.14 ± 0.70	0.203	5.11 ± 0.26	0.220	3.91 ± 0.28
0.261	4.44 ± 0.49	0.287	3.70 ± 0.48	0.266	3.30 ± 0.19	0.288	2.22 ± 0.19
0.331	1.788 ± 0.278	0.364	1.893 ± 0.307	0.337	2.03 ± 0.13	0.366	1.443 ± 0.140
0.408	0.866 ± 0.195	0.450	0.727 ± 0.183	0.417	1.201 ± 0.095	0.452	0.970 ± 0.107
0.490	0.349 ± 0.123			0.501	0.621 ± 0.069	0.544	0.530 ± 0.076
				0.592	0.387 ± 0.054	0.643	0.232 ± 0.056
				0.690	0.219 ± 0.044	0.751	0.083 ± 0.034
				0.796	0.114 ± 0.032	0.866	0.137 ± 0.038
				0.908	0.083 ± 0.028		
				1.027	0.081 ± 0.028		
a	$= 4.78 \pm 0.21$		3.78 ± 0.30		3.14 ± 0.20		2.96 ± 0.26
b	$= 12.33 \pm 0.79$		8.78 ± 1.00		7.67 ± 1.06		7.85 ± 1.26
c	$= ---$		---		1.24 ± 1.27		2.14 ± 1.35

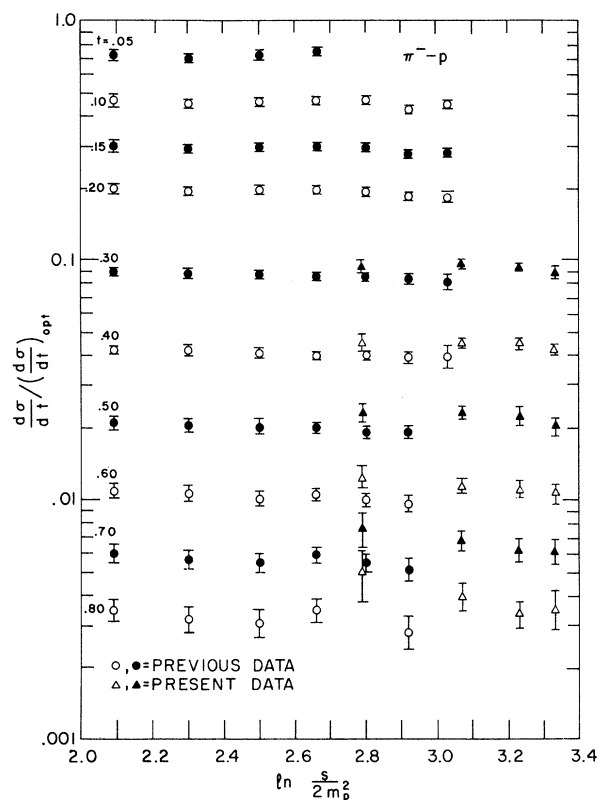
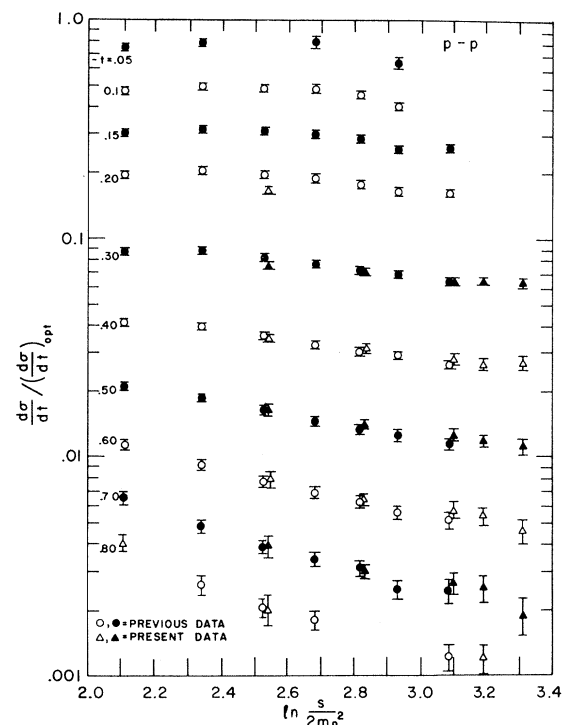


FIG. 3. $(d\sigma/dt)/(d\sigma/dt)_{\text{opt}}$ vs. $\ln(s/2m_p^2)$ (a) for p - p elastic scattering, including previous data; (b) for π^- - p elastic scattering, including previous data.

Table II. The coefficients for the fitted values of $\alpha(t)$.

$\alpha(t)$	
p - p	$(1.046 \pm 0.020) + (0.685 \pm 0.051)t$
π^- - p	$(0.982 \pm 0.030) - (0.062 \pm 0.068)t$
\bar{p} - p	$(0.900 \pm 0.084) - (0.914 \pm 0.376)t$
K^- - p	$(1.000 \pm 0.140) - (0.398 \pm 0.322)t$
p - p^a	$(0.963 \pm 0.080) + (0.378 \pm 0.193)t$
π^- - p^a	$(0.997 \pm 0.079) - (0.106 \pm 0.176)t$
π^+ - p^b	$(0.943 \pm 0.023) + (0.103 \pm 0.074)t$
K^+ - p^c	$(1.06 \pm 0.07) + (0.50 \pm 0.16)t$

^aUsing data above 14.8 BeV/c only.

^bSee reference 2.

^cSee reference 3.

previously obtained are also shown. Good fits to the energy dependence of the differential cross sections are obtained with a single Regge pole formula

$$d\sigma/dt = f(t) \exp\{[2\alpha(t) - 2] \ln s\},$$

where for each incident particle the values of $\alpha(t)$ can be fit with a linear function of t . While such a simple formula has little theoretical significance, it serves as a convenient parametrization of the data. The results obtained for α using both the present and earlier¹⁻³ data in the region of incident momentum 7 to 26 BeV/c are shown in Table II. We have also made this fit for π^- - p and p - p using only the data for incident momentum greater than 14.8 BeV/c. We see that the earlier conclusion, that the p - p diffraction peak shrinks, continues to hold to the highest energy studied. Although there is an indication of a reduction of the shrinkage effect with increasing energy, considering the errors, there is no good evidence for a change in behavior with increasing energy. The absence of shrinkage previously observed in the π^- - p case persists to the highest momentum (25 BeV/c). On the other hand, the \bar{p} - p cross sections [Fig. 2(c)] show steeper slopes than p - p and π^- - p and an expansion with increasing energy, the fit slope of $\alpha(t)$ vs t being somewhat more than 2.4 standard deviations from zero. The steep slope and consequently large radius associated with the \bar{p} - p interaction has also been observed at lower (~ 4 BeV/c) momenta.⁵ A comparison of values of α for K^+ - p ³ and K^- - p shows a difference in the slope of several standard deviations. For K^- - p we

find

$$\alpha = (1.00 \pm 0.14) - (0.40 \pm 0.32)t$$

and for K^+p

$$\alpha = (1.06 \pm 0.07) + (0.50 \pm 0.16)t.$$

As is well known by now, simple, reasonably convincing versions of the Regge pole theory do not fit the experimental data. Recently offered solutions⁶ involve so many arbitrary parameters that they are probably only of academic interest.

*Work performed under the auspices of the U. S. Atomic Energy Commission.

†Visitor from Rutherford High Energy Laboratory.

¹K. J. Foley, S. J. Lindenbaum, W. A. Love, S. Ozaki, J. J. Russell, and L. C. L. Yuan, Phys. Rev. Letters 10, 376 (1963); Nucl. Instr. and Meth. 30, 45 (1964).

²K. J. Foley, S. J. Lindenbaum, W. A. Love, S. Ozaki,

J. J. Russell, and L. C. L. Yuan, Phys. Rev. Letters 11, 425 (1963).

³K. J. Foley, S. J. Lindenbaum, W. A. Love, S. Ozaki, J. J. Russell, and L. C. L. Yuan, Phys. Rev. Letters 11, 503 (1963).

⁴In calculating $(d\sigma/dt)_{\text{opt}}$, total cross sections were taken from the following references: for $p-p$ and π^-p , G. von Dardel, D. Dekkers, R. Mermod, M. Vi-vargent, G. Weber, and K. Winter, Phys. Rev. Letters 8, 173 (1962); S. J. Lindenbaum, W. A. Love, J. A. Niederer, S. Ozaki, J. J. Russell, and L. C. L. Yuan, Phys. Rev. Letters 7, 184 (1961), 7, 352 (1961); for K^-p , W. F. Baker, R. L. Cool, E. W. Jenkins, T. F. Kycia, R. H. Phillips, and A. L. Read, Phys. Rev. 129, 2285 (1963); for $\bar{p}p$, S. J. Lindenbaum, W. A. Love, J. A. Niederer, S. Ozaki, J. J. Russell, and L. C. L. Yuan, Phys. Rev. Letters 7, 184 (1961).

⁵Y. Goldschmidt-Clermont et al., Proceedings of the International Conference on High-Energy Physics, Dubna, 1964 (to be published).

⁶W. Rarita and V. L. Teplitz, Phys. Rev. Letters 12, 206 (1964); T. O. Binford and B. P. Desai, Phys. Rev. 138, B1167 (1964).